PNAS
www.pnas.org

## Supporting Information for

# Facilitating hydrogen atom migration via a dense phase on palladium islands to a surrounding silver surface

Christopher R. O'Connor, Kaining Duanmu, Dipna A. Patel, Eri Muramoto, Matthijs A. van Spronsen, Dario Stacchiola, E. Charles H. Sykes, Philippe Sautet, Robert J. Madix, Cynthia M. Friend*

* Cynthia M. Friend

**Email:** friend@fas.harvard.edu

**This PDF file includes:**





www.pnas.org/cgi/doi/10.1073/pnas.2010413117

**Section S1. Temperature programmed experiments dosing enhancement correction**

The direct dosing enhancement has been accounted for in the temperature programmed desorption experiments in Figure 2 and Figure 3 separately because different dosing lines were used for each set of experiments. The direct dosing enhancement factor used in Figure 2 was determined by performing a background exposure of $3.0 \times 10^3$ L to a 0.45 ML palladium on Ag(111) surface at 150 K which gave the same yield ( ± 5 %) of dihydrogen as the curve reported in Figure 2. The direct dosing enhancement factor used in Figure 3 was determined by 1) estimating an approximate hydrogen atom coverage for 0.45 ML of palladium on Ag(111) by extrapolating the hydrogen atom coverage for a palladium coverage from Figure 3 and 2) estimating an approximate calibrated exposure for the coverage estimated above by extrapolating the dihydrogen exposure for a given hydrogen atom coverage from Figure 2. Since the direct dosing enhancement factor was not measured experimentally for Figure 3, the reported exposure of 50 L will have some error as a result of the two extrapolations necessary to calibrate the dose.

**Section S2. Kinetic analysis of dihydrogen desorption and comparison to theory**

The activation energy for dihydrogen desorption was estimated from the temperature programmed desorption spectra (Figures 2 – 3) by using second order desorption Redhead analysis (1) and assuming a pre-exponential factor of 0.13 $cm^2$ $molecules^{-1}$ $s^{-1}$, which was previously measured for hydrogen recombination from Pd(111) (2). The estimated activation energy for dihydrogen desorption from palladium islands on silver at 185 K is – 0.46 eV (– 44 KJ $mol^{-1}$) and at 240 K is – 0.68 eV (– 66 KJ $mol^{-1}$). The estimated activation energy for dihydrogen desorption from Pd(111) at 310 K is – 0.90 eV (– 87 KJ $mol^{-1}$) and at 370 K is – 1.00 eV (– 97 KJ $mol^{-1}$). Since there is no appreciable barrier for dissociation on palladium (3, 4), the difference in desorption temperature originating from palladium on palladium islands on Ag(111) at 240 K and on Pd(111) in the range of 310 – 370 K is due to more favorable adsorption of hydrogen atoms to Pd(111) by ~ 0.27 eV (26 KJ $mol^{-1}$). The weaker hydrogen atom adsorption on a single layer of palladium on Ag(111) versus multilayer Pd(111) is consistent with DFT calculations (Table S2). The calculated energetic difference of 0.28 eV (27 KJ $mol^{-1}$) between two hydrogen atoms adsorbed on Pd(111) versus a single layer of palladium on Ag(111) with the palladium lattice constant is in excellent agreement with the experimental measurements.

The adsorption energy is strongly dependent on the "extended" environment (e.g. neighbors, next nearest neighbors) which results in an energetic difference between Pd(111) and single-layer palladium on Ag(111) with the palladium lattice constant (Table S2). The vibrational frequency is highly dependent on the neighboring atoms as illustrated by the significant shift from 1050 to 800 $cm^{-1}$ when the lattice constant is expanded from that of palladium to silver for the overlayer model. The lack of a shift in the vibrational frequency suggests that the neighboring atom environment is nearly identical for multilayer Pd(111) versus the palladium overlayer on silver.

**Section S3. Temperature programmed desorption deconvolution and quantification**

A generic profile was used to determine the area of the desorption peaks because neither second- or first-order peak shape fit the data well (Figure S5). The peak profile was only used to determine area and the shape of the fit does not have any physical meaning. A Voigt profile gave ~5 % error in the peak area based on comparison to fits using first- and second-order desorption peak shapes. The fact that neither first- or second- order desorption profiles yield good fits indicates that the desorption behavior is complex.

In the quantitative analysis, the consideration of the molecular fragmentation pattern, ionization cross-section, and the mass spectrometer transmission and detection coefficients is necessary. It has been shown elsewhere (5) that the number density of molecule $i$ in the ionizer, $n_i$ , is given as follows:

$$n_i = \frac{\sigma_i^{-1} \cdot s_{ik}}{T_{ik} \cdot \delta_{ik}} \cdot \left(1 + \sum_j \frac{s_{ij}}{s_{ik}} \cdot \frac{T_{ik} \cdot \delta_{ik}}{T_{ij} \cdot \delta_{ij}}\right) \quad \textbf{(Equation S1)}$$

where

$\sigma_i$ is the total ionization cross-section of molecule $i$,

$s_{ik}$ is the measured signal current for the $k$th fragment of molecule $i$,

$s_{ij}/s_{ik}$ is the ratio of signals of the $j$th and $k$th fragments of molecule $i$ determined from separate calibrations of the neat parent molecule $i$,
$T_{ik}$ is the transmission coefficient of a fragment with m/z, $k$, of molecule $i$,
$T_{ij}$ is the transmission coefficient of a fragment with m/z, $j$, of molecule $i$,
$\delta_{ik}$ is the detection coefficient of a fragment with m/z, $k$, of molecule $i$,
$\delta_{ij}$ is the detection coefficient of a fragment with m/z, $j$, of molecule $i$.

In the equation above, the constants $\sigma_i$, $T_{ik}$, $T_{ij}$, $\delta_{ik}$ and $\delta_{ij}$ are taken from published values (Table S3). $s_{ij}/s_{ik}$ is determined for molecule i by introduction of a neat sample of molecule $i$ on to the vacuum chamber and the fragmentation pattern was recorded by QMS.

The absolute coverage of dihydrogen desorption is determined by quantitative mass spectrometry by calibration to the area of dioxygen desorption from a saturated p(4x4)O-Ag(111) surface which gives an oxygen coverage of 0.375 ML (6).

The local coverage of hydrogen atoms on silver is calculated by:

$$\theta_{\mathrm{H/Ag}} = \frac{\theta_{\mathrm{H}}^{185K}}{1-\theta_{\mathrm{Pd}}} \quad \textbf{(Equation S2)}$$

The local coverage of hydrogen atoms on palladium is calculated by:

$$\theta_{\mathrm{H/Pd}} = \frac{\theta_{\mathrm{H}}^{240K}}{\theta_{\mathrm{Pd}}} \quad \textbf{(Equation S3)}$$

**Section S4. Kinetic model for hydrogen atom migration**

We assume a simple kinetic model to quantitatively reproduce the effect of palladium coverage on the extent of hydrogen atom migration from palladium to silver. By assuming that a steady state concentration of hydrogen atoms on palladium is established during extended dihydrogen exposures and that availability of adsorption sites of hydrogen atoms on silver are not limiting, the rate of formation of hydrogen atoms on silver becomes dependent only on the concentration of hydrogen atoms on interfacial palladium. The following can be proven using the Polanyi-Wigner expression:

$$\frac{d\theta_{Ag}^{H}}{dt} = v \cdot \theta_{Pd-interface}^{H} \cdot e^{-\frac{E}{k_B T}} \quad \textbf{(Equation S4)}$$

Where $\theta_{Ag}^{H}$ is the coverage of hydrogen atoms on silver
$v$ is the pre-exponential factor
$\theta_{Pd-interface}^{H}$ is the coverage of hydrogen atoms on palladium at the palladium-silver interface
$E$ is the activation energy for diffusion
$k_B$ is Boltzmann's constant
$T$ is the sample temperature

By integrating over the length of a dihydrogen exposure, $t$, the following can be proven:

$$\theta_{Ag}^{H} = t \cdot v \cdot \theta_{Pd-interface}^{H} \cdot e^{-\frac{E}{k_B T}} \quad \textbf{(Equation S5)}$$

By assuming that the coverage of hydrogen atoms at the palladium-silver interface is proportional to the coverage of interfacial palladium, $\theta_{Pd-interface}$, by a factor, $b$, the following can be shown:

$$\theta_{Ag}^{H} = t \cdot v \cdot b \cdot \theta_{Pd-interface} \cdot e^{-\frac{E}{k_B T}} \quad \textbf{(Equation S6)}$$

By assuming that the coverage of hydrogen atoms on palladium is proportional to the coverage of palladium, $\theta_{Pd}$, by a factor, $c$, the ratio of hydrogen atoms on silver to palladiums is plotted in Figure 3C can be determined by:

$$\frac{\theta_{Ag}^{H}}{\theta_{Pd}^{H}} = \frac{t \cdot v \cdot b \cdot \theta_{Pd-interface} \cdot e^{-\frac{E}{k_B T}}}{\theta_{Pd} \cdot c} \quad \textbf{(Equation S7)}$$

A general constant, $A$, can be defined where:

$$\frac{\theta_{Ag}^{H}}{\theta_{Pd}^{H}} = A \cdot \frac{\theta_{Pd-interface}}{\theta_{Pd}};\ A = \frac{t \cdot v \cdot b \cdot e^{-\frac{E}{k_B T}}}{c} \quad \textbf{(Equation S8)}$$

The coverage of hydrogen atoms at the palladium-silver interface can be estimated by assuming hexagonal island growth with increasing palladium coverage. The approximate number

of palladium atoms in a hexagonal palladium island with a side to side diameter, $d$, and Pd-Pd distance, $r_{Pd-Pd}$, is given by:

$$n_{Pd} = \frac{Area}{Unit\ cell\ area} = \frac{\frac{\sqrt{3}\,d^2}{2}}{r_{Pd-Pd}^2 \sin(60^o)} = \frac{\frac{\sqrt{3}\,d^2}{2}}{(0.225\ nm)^2 \sin(60^o)} \quad \textbf{(Equation S9)}$$

The approximate number of interfacial palladium atoms in a hexagonal palladium island with a side to side radius, $r$, and Pd-Pd distance, $r_{Pd-Pd}$, is given by:

$$n_{Pd-interface} = \frac{Circumference}{r_{Pd-Pd}} = \frac{\frac{6\,d}{\sqrt{3}}}{r_{Pd-Pd}} = \frac{\frac{6\,d}{\sqrt{3}}}{0.225\ nm} \quad \textbf{(Equation S10)}$$

The palladium interface concentration can then be calculated by:

$$\theta_{Pd-interface} = \frac{n_{Pd-interface}}{n_{Pd}} = \frac{\frac{6\,d}{\sqrt{3}}}{0.225\ nm} \cdot \frac{(0.225\ nm)^2 \sin(60^o)}{\frac{\sqrt{3}\,d^2}{2}} \quad \textbf{(Equation S11)}$$

By substituting, Equation S11 into Equation S8 the following can be shown:

$$\frac{\theta_{Ag}^H}{\theta_{Pd}^H} = A \cdot \frac{\frac{6\,d}{\sqrt{3}}}{0.225\ nm} \cdot \frac{(0.225\ nm)^2 \sin(60^o)}{\frac{\sqrt{3}\,d^2}{2}} \cdot \frac{1}{\theta_{Pd}} \quad \textbf{(Equation S12)}$$

By substituting, the relationship established between palladium island side to side diameter and palladium coverage stablished in Figure S2, the following can be shown:

$$\frac{\theta_{Ag}^H}{\theta_{Pd}^H} = A \cdot \frac{\frac{6\cdot(9.66\cdot\sqrt{\theta_{Pd}})}{\sqrt{3}}}{0.225\ nm} \cdot \frac{(0.225\ nm)^2 \sin(60^o)}{\frac{\sqrt{3}\cdot(9.66\cdot\sqrt{\cdot\theta_{Pd}})^2}{2}} \cdot \frac{1}{\theta_{Pd}} \quad \textbf{(Equation S13)}$$

The best fit for the experimental data in Figure 3C yielded $A = 4.7$ and is plotted in Figure 3C.

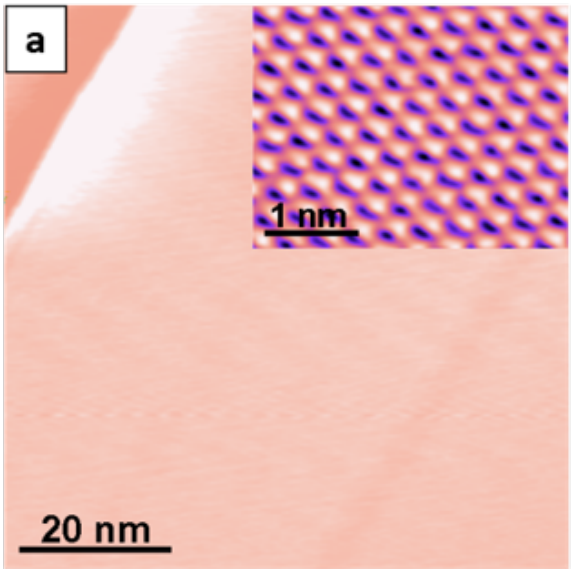


**Figure S1.** Morphology of Ag(111) as determined by STM experiments. (A) A largely defect free Ag(111) surface with a monoatomic step edge. Inset depicts an atomic-resolution image of Ag(111) terrace.

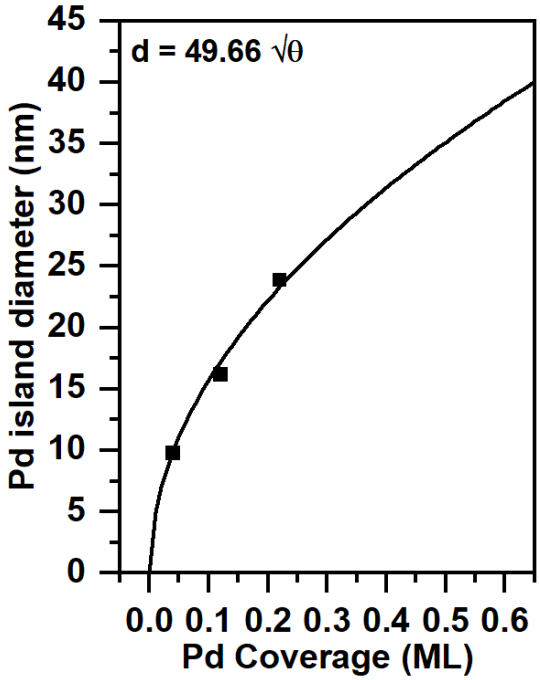


**Figure S2.** Palladium island side to side diameter dependence on palladium coverage fit with a square root function which is expected for island growth where palladium adds to existing islands. This assumption was shown to be accurate by STM experiments.

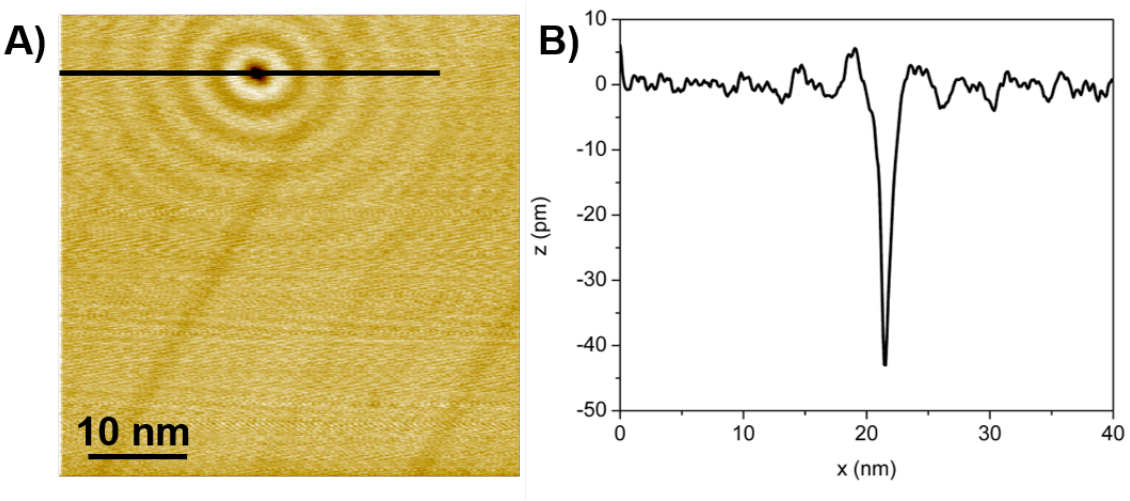


**Figure S3.** The presence of impurities in Ag(111) yield features with apparent depths that are distinct from hydrogen atoms as determined by STM experiments. (A) STM image of a clean Ag(111) crystal with an impurity ( the Ag(111) crystal had on average < 1 impurity per 50 × 50 $nm^2$). (B) Apparent height profile along the black line scan in (A) shows the impurity has an apparent depth of ~ 50 pm.

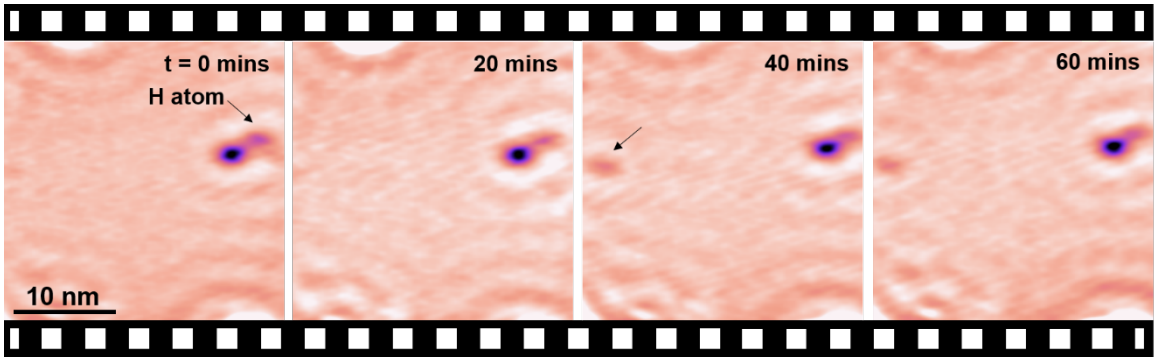


**Figure S4.** Hydrogen atoms diffuse on Ag(111) at 5 K via quantum tunneling. Frames from an STM time-lapse movie depict hydrogen atoms (H atoms) diffusing on silver on a 0.05 ML of palladium on Ag(111) surface. The arrow indicates diffusion of a hydrogen atom due to quantum tunneling. Imaging conditions: 0.030 V, 0.020 nA, 5 K.

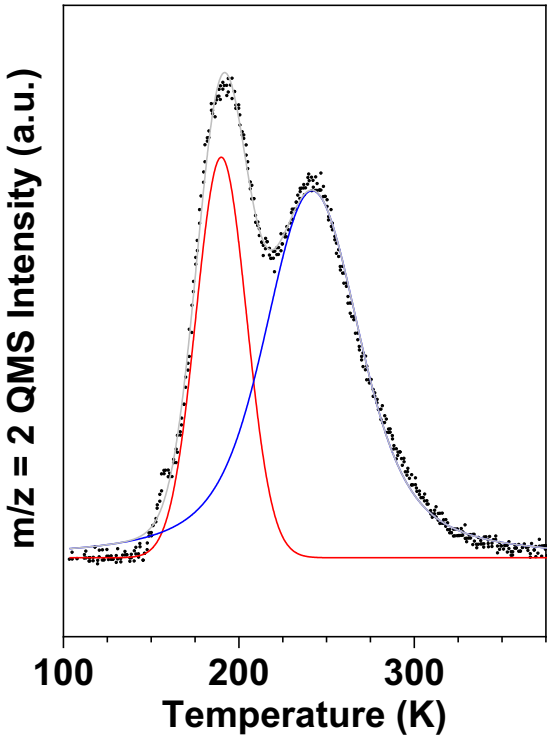


**Figure S5.** Deconvolution of the TPD spectra for a 180000 L exposure of dihydrogen to 0.45 ML of palladium on Ag(111) at 150 K in Figure 2A.

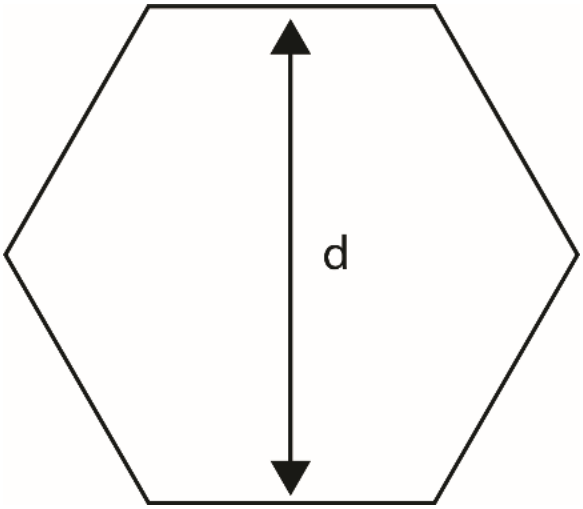


**Figure S6.** Hexagon model for palladium islands.

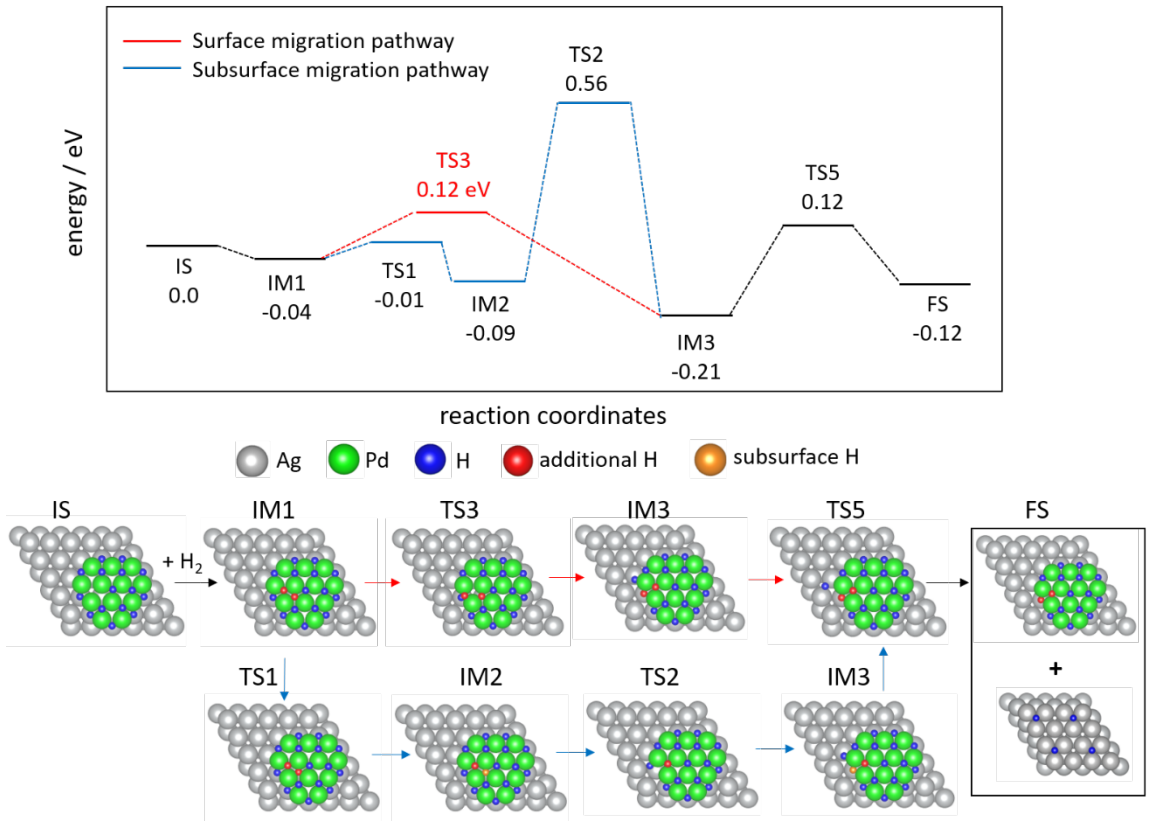


**Figure S7.** Reaction pathway for hydrogen migration on a $Pd_{12}$ island at high hydrogen atom coverage (silver: silver atom; green: palladium atom; blue: initially adsorbed hydrogen atom; red: additional surface hydrogen atom from dihydrogen; yellow: hydrogen atom in the subsurface). The $Pd_{12}$ island was fully covered by atomic hydrogen except one fcc vacancy (IS). After dihydrogen adsorption, one hydrogen atom goes to a fcc site and one hydrogen atom goes to a nearby hcp site (IM1). The hydrogen atom on the hcp site can migrate to Ag(111) through a surface pathway (red) or a subsurface pathway (blue).

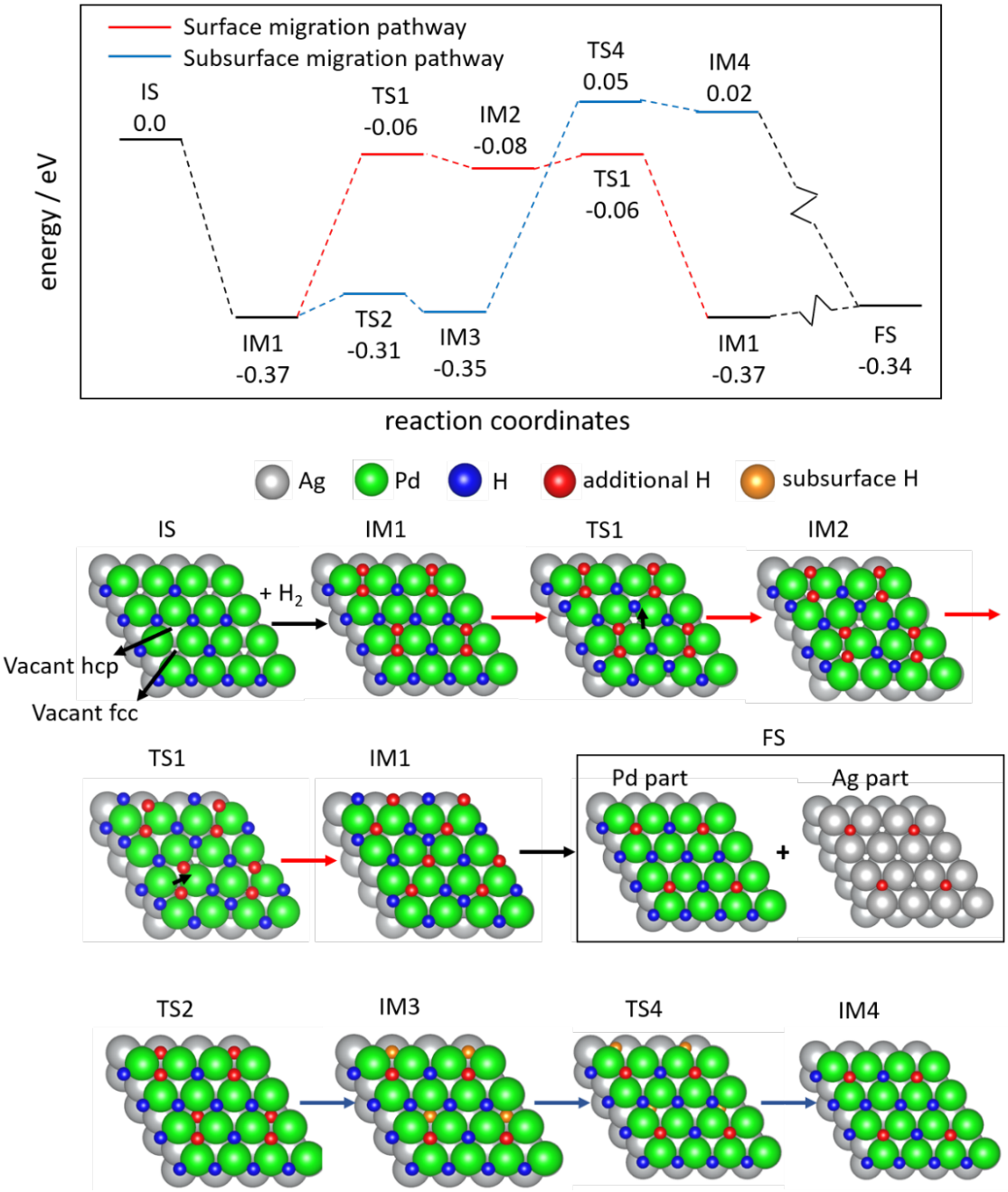


**Figure S8.** A reaction pathway for dihydrogen dissociation and hydrogen atom migration on a palladium overlayer on Ag(111) at high hydrogen atom coverage for both surface (top) and subsurface (bottom) migration (silver: silver atom; green: palladium atom; blue: initially adsorbed hydrogen atom; red: additional surface hydrogen atom from dihydrogen; yellow: hydrogen atom in the subsurface). The surface was initially covered by 0.75 ML of hydrogen atoms (pink)(IS), after further dihydrogen adsorption, additional hydrogen atoms (red) occupy a fcc site and an hcp site (IM1). The hydrogen atom on a hcp site can move on the surface (red arrow) via a bridge site (TS2) or to a position under the surface (blue pathway)(IM2), and eventually migrate to the Ag(111) surface (FS). Since the hydrogen atom coverage is high, the silver lattice periodicity was used for the palladium overlayer (see text). All energies are given per $H_2$ unit, referred to $H_2$ in the gas phase.

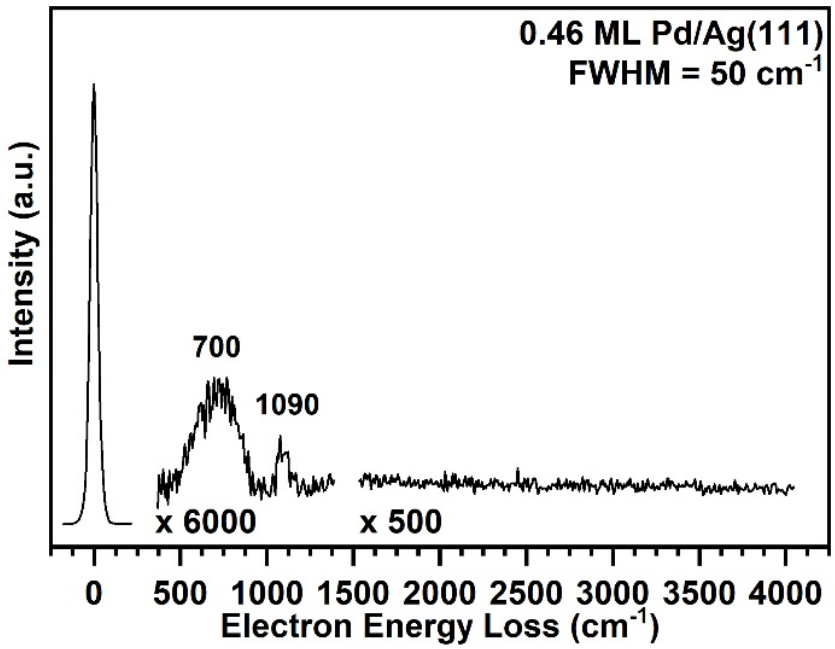


**Figure S9.** Vibrational spectroscopy demonstrates the dissociation of dihydrogen on a thin film of palladium on Ag(111). A background adsorption of dihydrogen (150 K, 1 L) on 0.46 ML of palladium on Ag(111) leads to the sole adsorption of hydrogen atoms on palladium and no adsorption of common background gases such as carbon monoxide and water.

**Table S1.** STM statistical analysis for 0.04, 0.12 and 0.22 ML of palladium on Ag(111)

| Palladium coverage (ML) | Palladium diameter (nm) | Single layer island height (pm) | Multilayer island height (pm) | Multilayer island coverage[a] (%) |
|---|---|---|---|---|
| 0.04 | 9.8 ± 1.5 | 144.7 ± 8.2 | - | - |
| 0.12 | 16.2 ± 2.5 | 141.3 ± 7.7 | 276.7 ± 20.3 | 1.05 |
| 0.22 | 23.9 ± 4.3 | 141.4 ± 7.9 | 416.0 ± 21.0 | 2.20 |

[a] Coverage determined with respect to the total surface area

**Table S2.** Hydrogen atom adsorption energies[a] and vibrational frequencies determined by DFT calculations

| Surface | H coverage (ML) | H adsorption energy[a] (eV / KJ $mol^{-1}$) | H-Pd perpendicular vibrational frequency ($cm^{-1}$) |
|---|---|---|---|
| Pd overlayer on Ag(111) (Pd lattice constant) | 1 ML | – 0.84 / – 81 | 1050 |
| Pd overlayer on Ag(111) (Ag lattice constant) | 1 ML | – 1.12 / – 108 | 800 |
| Pd(111) | 1 ML | – 1.12 / – 108 | 1046 |

[a] All adsorption energies are for two adsorbed hydrogen atoms with respect to $H_2$ in the gas phase. The reported adsorption energies are an average energy for two adsorbed hydrogen atoms between the initial atomic hydrogen coverage of 0 ML and the final coverage of 1 ML

**Table S3.** Mass spectrometry quantitative analysis constants

| m/z | Transmission Coefficient [a] | Detection Coefficient [b] | Molecule | Ionization Cross-section |
|---|---|---|---|---|
| 0-20 | 1 | 1.5 | $H_2$ | 1.021[c] |
| 21-30 | 1 | 1 | $O_2$ | 2.441[c] |
| 31-40 | 1 | 0.9 | | |

[a] Adapted from Hiden manual

[b] Adapted from UTI manual

[c] Values calculated at an incident electron voltage of 70 eV from the NIST database

**Table S4.** Absolute and local coverages of hydrogen atoms on palladium and silver determined in Figure 2

| | $H_2$ desorption at 185 K | | $H_2$ desorption at 240 K | |
|---|---|---|---|---|
| $H_2$ Exposure (L) | $\theta_{\mathrm{H}}^{185K}$ (ML) | $\theta_{\mathrm{H/Ag}}$ (ML) | $\theta_{\mathrm{H}}^{240K}$ (ML) | $\theta_{\mathrm{H/Pd}}$ (ML) |
| 5.9 | 0.00 ± 0.01 | 0.00 ± 0.01 | 0.234 ± 0.02 | 0.519 ± 0.05 |
| $5.9 \times 10^1$ | 0.030 ± 0.01 | 0.06 ± 0.02 | 0.257 ± 0.03 | 0.570 ± 0.06 |
| $6.0 \times 10^2$ | 0.104 ± 0.02 | 0.19 ± 0.03 | 0.303 ± 0.03 | 0.674 ± 0.07 |
| $3.0 \times 10^3$ | 0.228 ± 0.03 | 0.41 ± 0.04 | 0.383 ± 0.04 | 0.850 ± 0.08 |
| $1.8 \times 10^6$ | 0.308 ± 0.03 | 0.56 ± 0.06 | 0.473 ± 0.05 | 1.051 ± 0.10 |

5

**Table S5.** Absolute and local coverages of hydrogen atoms on palladium and silver determined in Figure 3.

| | $H_2$ desorption at 185 K | | $H_2$ desorption at 240 K | |
|---|---|---|---|---|
| Pd coverage (ML) | $\theta_H^{185K}$ (ML) | $\theta_{H/Ag}$ (ML) | $\theta_H^{240K}$ (ML) | $\theta_{H/Pd}$ (ML) |
| 0.05 | 0.011 ± 0.01 | 0.013 ± 0.01 | 0.023 ± 0.01 | 0.462 ± 0.05 |
| 0.15 | 0.013 ± 0.01 | 0.016 ± 0.01 | 0.072 ± 0.01 | 0.483 ± 0.05 |
| 0.25 | 0.017 ± 0.01 | 0.023 ± 0.01 | 0.128 ± 0.01 | 0.512 ± 0.05 |
| 0.35 | 0.020 ± 0.01 | 0.031 ± 0.02 | 0.174 ± 0.02 | 0.496 ± 0.05 |
| 0.55 | 0.027 ± 0.01 | 0.059 ± 0.02 | 0.319 ± 0.03 | 0.579 ± 0.06 |

5

**References**


1. P. A. Redhead, Thermal desorption of gases. *Vacuum* **12**, 203–211 (1962).

2. R. J. Madix, G. Ertl, K. Christmann, Preexponential Factors for Hydrogen Desorption from Single Crystal Metal Surfaces. *Chemical Physics Letters* **62**, 38–41 (1979).

3. T. Mitsui, M. K. Rose, E. Fomin, D. F. Ogletree, M. Salmeron, Dissociative hydrogen adsorption on palladium requires aggregates of three or more vacancies. *Nature* **422**, 705–707 (2003).

4. T. Mitsui, M. K. Rose, E. Fomin, D. F. Ogletree, M. Salmeron, Hydrogen adsorption and diffusion on Pd(1 1 1). *Surface Science* **540**, 5–11 (2003).

5. B. Xu, R. J. Madix, C. M. Friend, Achieving optimum selectivity in oxygen assisted alcohol cross-coupling on gold. *Journal of the American Chemical Society* **132**, 16571–16580 (2010).

6. A. Klust, R. J. Madix, Mesoscopic restructuring and mass transport of metal atoms during reduction of the Ag (111) -p (4×4) -O surface with CO. *Journal of Chemical Physics* **126**, 084707 (2007).